Available online at www.sciencedirect.com
SCIENCE DIRECT®
Journal of Solid State Chemistry 170 (2003) 203–210
JOURNAL OF SOLID STATE CHEMISTRY
http://elsevier.com/locate/jssc

Crystal growth, structure determination, and optical properties of new potassium-rare-earth silicates $K_3RESi_2O_7$ (RE = Gd, Tb, Dy, Ho, Er, Tm, Yb, Lu)

Ioana Vidican, Mark D. Smith, and Hans-Conrad zur Loye*

Department of Chemistry and Biochemistry, University of South Carolina, 631 Sumter Street, Columbia, SC 29208, USA

Received 30 April 2002; received in revised form 15 August 2002; accepted 27 August 2002

Abstract

Single crystals of $K_3RESi_2O_7$ (RE = Gd, Tb, Dy, Ho, Er, Tm, Yb, Lu) were grown from a potassium fluoride flux. Two different structure types were found for this series. Silicates containing the larger rare earths, RE = Gd, Tb, Dy, Ho, Er, Tm, Yb crystallize in a structure $K_3RESi_2O_7$ that contains the rare-earth cation in both a slightly distorted octahedral and an ideal trigonal prismatic coordination environment, while in $K_3LuSi_2O_7$, containing the smallest of the rare earths, lutetium is found solely in an octahedral coordination environment. The structure of $K_3LuSi_2O_7$ crystallizes in space group $P6_3/mmc$ with $a = 5.71160(10)$ Å and $c = 13.8883(6)$ Å. The structures containing the remaining rare earths crystallize in the space group $P6_3/mcm$ with the lattice parameters of $a = 9.9359(2)$ Å, $c = 14.4295(4)$ Å, ($K_3GdSi_2O_7$); $a = 9.88730(10)$ Å, $c = 14.3856(3)$ Å, ($K_3TbSi_2O_7$); $a = 9.8673(2)$ Å, $c = 14.3572(4)$ Å, ($K_3DySi_2O_7$); $a = 9.8408(3)$ Å, $c = 14.3206(6)$ Å, ($K_3HoSi_2O_7$); $a = 9.82120(10)$ Å, $c = 14.2986(2)$ Å, ($K_3ErSi_2O_7$); $a = 9.80200(10)$ Å, $c = 14.2863(4)$ Å, ($K_3TmSi_2O_7$); $a = 9.78190(10)$ Å, $c = 14.2401(3)$ Å, ($K_3YbSi_2O_7$). The optical properties of the silicates were investigated and $K_3TbSi_2O_7$ was found to fluoresce in the visible.

Keywords: Alkali-metal-rare-earth silicates; Fluorescence; $K_3G_dSi_2O_7$; $K_3Tbsi_2O_7$; $K_3DySi_2O_7$; $K_3HoSi_2O_7$; $3ErSi_2O_7$; $K_3TmSi_2O_7$; $K_3YbSi_2O_7$; $K_3LuSi_2O_7$

1. Introduction

Silicates represent one of the largest groups of oxides and many are found naturally as minerals, often in single-crystal form. A significant exception are the rare-earth silicates, which do not occur as "pure" phases in nature, due to the nearly identical size and chemistry of the rare earths. Minerals of rare earths typically contain mixtures of rare earths and, consequently, the systematic investigation of rare-earth silicates had to await the availability of pure rare-earth reagents. In the late 1950s, numerous investigations of rare-earth silicates were undertaken and for the simple binaries, RE_2O_3–SiO_2, compounds with compositions 1:1, 7:9, and 1:2 were synthesized and structurally characterized [1–5]. Within this group of rare-earth silicates, the lanthanide coordination ranges between six and ten and crystal structures can contain isolated SiO_4 tetrahedra or groups of Si_2O_7 or Si_3O_{10}. This work was reviewed by Felsche [6], who discussed the relationship between structure and rare-earth size extensively. To date, eight distinct structure types for the binary rare-earth silicates are known [7].

A number of ternary alkali-rare-earth silicates are known, including $NaRE(SiO_4)$, $Na_3RESi_2O_7$ [8–11], $K_3NdSi_6O_{15}$ [12], $K_6Lu_2Si_6O_{18}$ [13], $K_6Tm_2Si_6O_{18}$ [14], $K_3NdSi_7O_{17}$ [15], $K_5NdSi_9O_{22}$, $K_3NdSi_6O_{15}$, $K_3NdSi_6O_{15}$ [16], and $K_3HoSi_3O_9$ [17]. In addition to the ternary compounds with the composition $Na_3RESi_2O_7$, two potassium analogues, $K_3EuSi_2O_7$ [18] and $K_3NdSi_2O_7$, [19] are known and have been structurally characterized. The structure type of the sodium containing rare-earth disilicates is a common one, often observed during hydrothermal synthesis in systems Na_2O–RE_2O_3–SiO_2–H_2O [8,9]. While the $Na_3RESi_2O_7$ structures are similar

*Corresponding author. Fax: +1-803-7778508.
E-mail address: zurloye@sc.edu (H.-C. zur Loye).

0022-4596/03/$ - see front matter © 2002 Elsevier Science (USA). All rights reserved.
PII: S0022-4596(02)00029-4

to the potassium containing analogues, they typically crystallize in lower symmetry hexagonal space groups.

Previous attempts by other groups to grow rare-earth silicate crystals from alkali fluoride fluxes MF (M = Li, Na, K) indicated that KF as a flux is superior to both LiF and NaF [20], since crystals grown from KF were typically better formed and obtained in greater yield. We have, consequently, used KF as a flux to investigate the crystal growth of rare-earth silicates and prepared a series of new alkali-rare-earth silicates, $K_3RESi_2O_7$ (RE = Gd, Tb, Dy, Ho, Er, Tm, Yb, Lu). We have determined the structures of these new potassium-rare-earth silicates and have investigated their optical properties. Our findings are reported within this paper.

2. Experimental

2.1. Crystal growth

Single crystals of $K_3RESi_2O_7$ (RE = Gd, Tb, Dy, Ho, Er, Tm, Yb, Lu) were grown by heating stoichiometric quantities of the rare-earth oxide (REacton, 99.9%) and silicon oxide (Alfa-Aesar, 99.9%) with a ten-fold excess of potassium fluoride (Alfa-Aesar, 99.9%). The oxides, typically 1 g, and the flux, typically 10 g, were placed in a platinum crucible covered with a platinum lid. The crucibles were heated in air at 1100°C for 10 h followed by slow cooling, 3°/h, to 800°C and subsequent cooling to room temperature by turning off the furnace. The crystals were removed from the flux matrix by washing with warm water and sonication.

2.2. Scanning electron microscopy

Scanning electron micrographs of several single crystals were obtained using a Philips XL 30 ESEM instrument utilized in the environmental mode. An ESEM image of a typical crystal is shown in Fig. 1. The ESEM also confirmed the presence of potassium, the rare earth, silicon, and oxygen in the $K_3RESi_2O_7$ crystals and, within the detection limit of the instrument, verified the absence of other elements, such as platinum or fluorine, in the crystals.

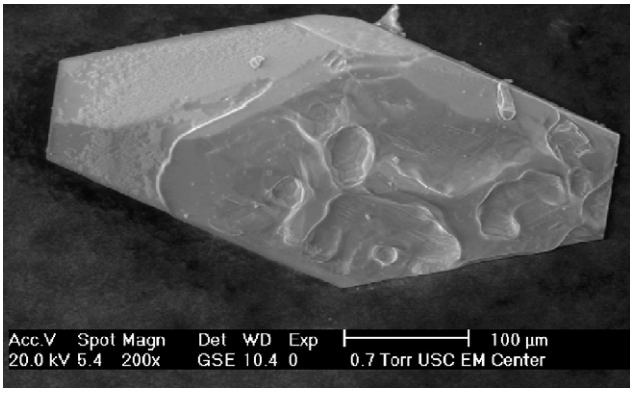

Fig. 1. ESEM image of a flux-grown $K_3TbSi_2O_7$ crystal.

2.3. Structure determination

For the structure determination of $K_3RESi_2O_7$ (RE = Gd, Tb, Dy, Ho, Er, Tm, Yb, Lu), colorless (Gd, Tb, Dy, Tm, Yb, Lu), pale yellow (Ho) or pink (Er) multifaceted prisms were epoxied onto the end of thin glass fibers. X-ray intensity data were measured in ω scan mode at 293 K on a Bruker SMART APEX CCD-based diffractometer system (Mo$K\alpha$ radiation, $\lambda = 0.71073$ A) [21].

After determination of crystal quality and initial hexagonal unit-cell parameters, raw data frames of width 0.3° in ω were measured to $2\theta_{max} \geqslant 70°$ (completeness $\geqslant$ 99.5%, average redundancy >9). Exposure time per frame ranged from 5 to 20 s for the different samples. The raw data frames were integrated with SAINT+, [21] which also applied corrections for Lorentz and polarization effects. The final unit-cell parameters for each compound are based on the least-squares refinement of all reflections with $I > 5\sigma(I)$ from each data set. Analyses of the data showed negligible crystal decay during data collection for all samples. An empirical absorption correction based on the multiple measurement of equivalent reflections was applied to each data set with the program SADABS [21].

Systematic absences in the intensity data were consistent with the space group $P6_3/mmc$ ($K_3LuSi_2O_7$) and $P6_3/mcm$ ($K_3RESi_2O_7$ (Gd, Tb, Dy, Ho, Er, Tm, Yb). The structures were solved by a combination of direct methods and difference Fourier syntheses, and refined by full-matrix least-squares against F^2, using the SHELXTL software package [22]. All atoms were refined with anisotropic displacement parameters. No significant deviation from unit occupancy was observed for any of the atoms in any of the structures.

Relevant crystallographic information is detailed in Table 1, the atomic coordinates are listed in Table 2, and selected interatomic distances and angles are listed in Table 3.

2.4. Fluorescence measurements

Fluorescence measurements were performed on a Model 8100 SLM-AMINCO spectrofluorometer with excitation at 350 and 4 nm slits using a single crystal mounted on a glass fiber.

Table 1
Summary of crystallographic data and least-squares refinement results for $K_3RESi_2O_7$ (RE = Gd, Tb, Dy, Ho, Er, Tm, Yb, Lu)

Compound	$K_3GdSi_2O_7$	$K_3TbSi_2O_7$	$K_3DySi_2O_7$	$K_3HoSi_2O_7$	$K_3ErSi_2O_7$	$K_3TmSi_2O_7$	$K_3YbSi_2O_7$	$K_3LuSi_2O_7$
Formula weight	442.73	444.40	447.98	450.41	452.74	454.41	458.52	460.45
Space group	$P6_3/mcm$	$P6_3/mcm$	$P6_3/mcm$	$P6_3/mcm$	$P6_3/mcm$	$P6_3/mcm$	$P6_3/mcm$	$P6_3/mmc$
a (Å)	9.9359(2)	9.88730(10)	9.8673(2)	9.8408(3)	9.82120(10)	9.80200(10)	9.78190(10)	5.71160(10)
c (Å)	14.4295(4)	14.3856(3)	14.3572(4)	14.3206(6)	14.2986(2)	14.2863(4)	14.2401(3)	13.8883(6)
V (Å^3)	1233.66(5)	1217.91(3)	1210.59(5)	1200.93(7)	1194.41(2)	1188.72(4)	1180.02(3)	392.37(2)
Z	6	6	6	6	6	6	6	2
Crystal shape	Multifaceted prism	Multifaceted prism	Multifaceted prism	Multifaceted prism	Multifaceted prism	Multifaceted Prism	Multifaceted Prism	Irregular
Crystal size (mm)	$0.22 \times 0.15 \times 0.12$	$0.18 \times 0.16 \times 0.08$	$0.18 \times 0.12 \times 0.06$	$0.22 \times 0.16 \times 0.12$	$0.24 \times 0.18 \times 0.10$	$0.18 \times 0.08 \times 0.06$	$0.08 \times 0.05 \times 0.03$	$0.08 \times 0.06 \times 0.04$
Reflections collected	14,770	15,640	11,647	13,629	14,711	15,696	14,796	4688
Independent reflections	1113 [R(int) = 0.0330]	1668 [R(int) = 0.0510]	1402 [R(int) = 0.0365]	1192 [R(int) = 0.0413]	1387 [R(int) = 0.0387]	1378 [R(int) = 0.0350]	1781 [R(int) = 0.0396]	373 [R(int) = 0.0463]
Data/restrains/ parameters	1113/0/41	1668/0/41	1402/0/41	1192/0/41	1387/0/41	1378/0/41	1781/0/40	373/0/19
Goodness-of-fit on F^2	1.071	1.032	1.082	1.217	1.234	1.043	1.039	1.187
Final R indices $R1$	0.0231	0.0279	0.0255	0.0297	0.0298	0.0230	0.0343	0.0425
[$I > 2$sigma(I)]	0.0628	0.0636	0.0615	0.0688	0.0722	0.0558	0.0792	0.0848
w$R2$								
Largest diff. peak and hole	1.366 and – 1.890 e Å^{-3}	2.848 and – 2.198 e Å^{-3}	0.975 and – 1.535 e Å^{-3}	1.684 and – 2.174 e Å^{-3}	2.281 and – 1.858 e Å^{-3}	1.815 and – 1.428 e.Å^{-3}	5.149 and – 1.957 e.Å^{-3}	1.668 and – 4.375 e.Å^{-3}

Table 2
Atomic coordinates and equivalent isotropic displacement parameters ($Å^2 \times 10^3$) for $K_3RESi_2O_7$ (RE = Gd–Lu)

	Wyck	X	Y	Z	U (eq)		Wyck	X	Y	Z	U (eq)
$K_3GdSi_2O_7$						*$K_3TbSi_2O_7$*					
K(1)	12*k*	0.3311(1)	0	0.0910(1)	18(1)	K(1)	12*k*	0.3313(1)	0	0.0913(1)	18(1)
K(2)	4*c*	1/3	2/3	1/4	16(1)	K(2)	4*c*	1/3	2/3	1/4	16(1)
K(3)	2*b*	0	0	0	15(1)	K(3)	2*b*	0	0	0	15(1)
Gd(1)	4*d*	1/3	2/3	0	6(1)	Tb(1)	4*d*	1/3	2/3	0	6(1)
Gd(2)	2*a*	0	0	1/4	6(1)	Tb(2)	2*a*	0	0	1/4	6(1)
Si(1)	12*k*	0.6585(1)	0	0.1434(1)	6(1)	Si(1)	12*k*	0.6583(1)	0	0.1432(1)	6(1)
O(1)	24*l*	0.6781(2)	0.5241(2)	0.9069(1)	14(1)	O(1)	24*l*	0.6785(2)	0.5239(2)	0.9074(1)	13(1)
O(2)	12*k*	0.8218(2)	0	0.1463(1)	12(1)	O(2)	12*k*	0.8223(2)	0	0.1464(1)	11(1)
O(3)	6*g*	0.5955(2)	0	1/4	13(1)	O(3)	6*g*	0.5944(3)	0	1/4	12(1)
$K_3DySi_2O_7$						*$K_3HoSi_2O_7$*					
K(1)	12*k*	0.3315(1)	0	0.0916(1)	18(1)	K(1)	12*k*	0.3315(1)	0	0.0919(1)	18(1)
K(2)	4*c*	1/3	2/3	$\frac{1}{4}$	16(1)	K(2)	4*c*	1/3	2/3	1/4	16(1)
K(3)	2*b*	0	0	0	15(1)	K(3)	2*b*	0	0	0	16(1)
Dy(1)	4*d*	1/3	2/3	0	6(1)	Ho(1)	4*d*	1/3	2/3	0	6(1)
Dy(2)	2*a*	0	0	$\frac{1}{4}$	6(1)	Ho(2)	2*a*	0	0	1/4	6(1)
Si(1)	12*k*	0.6580(1)	0	0.1431(1)	6(1)	Si(1)	12*k*	0.6573(1)	0	0.1429(1)	6(1)
O(1)	24*l*	0.6781(2)	0.5234(2)	0.9077(1)	13(1)	O(1)	24*l*	0.6786(2)	0.5234(2)	0.9080(1)	12(1)
O(2)	12*k*	0.8226(2)	0	0.1469(1)	11(1)	O(2)	12*k*	0.8226(3)	0	0.1473(2)	11(1)
O(3)	6*g*	0.5937(3)	0	$\frac{1}{4}$	12(1)	O(3)	6*g*	0.5929(4)	0	1/4	11(1)
$K_3ErSi_2O_7$						*$K_3TmSi_2O_7$*					
K(1)	12*k*	0.3316(1)	0	0.0920(1)	19(1)	K(1)	12*k*	0.3318(1)	0	0.0923(1)	17(1)
K(2)	4*c*	1/3	2/3	$\frac{1}{4}$	16(1)	K(2)	4*c*	1/3	2/3	1/4	15(1)
K(3)	2*b*	0	0	0	17(1)	K(3)	2*b*	0	0	0	15(1)
Er(1)	4*d*	1/3	2/3	0	7(1)	Tm(1)	4*d*	1/3	2/3	0	6(1)
Er(2)	2*a*	0	0	$\frac{1}{4}$	7(1)	Tm(2)	2*a*	0	0	1/4	6(1)
Si(1)	12*k*	0.6574(1)	0	0.1429(1)	7(1)	Si(1)	12*k*	0.6574(1)	0	0.1427(1)	6(1)
O(1)	24*l*	0.6783(2)	0.5227(2)	0.9082(1)	14(1)	O(1)	24*l*	0.684(2)	0.5225(2)	0.9087(1)	12(1)
O(2)	12*k*	0.8229(2)	0	0.1475(1)	12(1)	O(2)	12*k*	0.8232(2)	0	0.1478(1)	10(1)
O(3)	6*g*	0.5919(3)	0	$\frac{1}{4}$	12(1)	O(3)	6*g*	0.5914(3)	0	1/4	11(1)
$K_3YbSi_2O_7$						*$K_3LuSi_2O_7$*					
K(1)	12*k*	0.3317(1)	0	0.0924(1)	17(1)	K(1)	8*h*	1/3	2/3	0.0922(2)	16(1)
K(2)	4*c*	1/3	2/3	$\frac{1}{4}$	16(1)	K(2)	2*a*	0	0	1/4	21(1)
K(3)	2*b*	0	0	0	18(1)						
Yb(1)	4*d*	1/3	2/3	0	6(1)	Lu(1)	2*b*	0	0	0	9(1)
Yb(2)	2*a*	0	0	$\frac{1}{4}$	7(1)						
Si(1)	12*k*	0.6572(1)	0	0.1425(1)	6(1)	Si(1)	8*h*	2/3	1/3	0.1317(2)	7(1)
O(1)	24*l*	0.6784(3)	0.5221(2)	0.9090(1)	12(1)	O(1)	24*l*	0.3596(11)	0.1798(5)	0.0961(4)	15(1)
O(2)	12*k*	0.8232(3)	0	0.1477(2)	11(1)	O(2)	4*c*	2/3	1/3	1/4	33(4)
O(3)	6*g*	0.5913(4)	0	$\frac{1}{4}$	12(1)						

U_{eq} is defined as one-third of the trace of the orthogonalized U_{ij} tensor.

3. Results and discussion

3.1. The crystal structures

Clear multifaceted crystals of $K_3RESi_2O_7$ (RE = Gd, Tb, Dy, Ho, Er, Tm, Yb, Lu) were grown from a potassium fluoride flux, where the flux acted as both melt and reactant. Typical crystals were approximately 0.5 mm in size, and a representative ESEM image of $K_3TbSi_2O_7$ is shown in Fig. 1. The ESEM also verified the presence of potassium, terbium, silicon, and oxygen for the $K_3TbSi_2O_7$ crystals. No extraneous elements were detected in the crystals.

Two different crystal structures were found in the series $K_3RESi_2O_7$ (RE = Gd, Tb, Dy, Ho, Er, Tm, Yb, Lu). $K_3RESi_2O_7$ (RE = Gd, Tb, Dy, Ho, Er, Tm, and Yb) crystallize in the space group $P6_3/mcm$, while $K_3LuSi_2O_7$ crystallizes in space group $P6_3/mmc$.

Silicate structures can contain isolated SiO_4 tetrahedra or groups of Si_2O_7 or Si_3O_{10} [6]. The structure of $K_3RESi_2O_7$, Fig. 2, contains columns of Si_2O_7 groups along the crystallographic c-direction that are connected to the rare-earth cations to form a three-dimensional framework. The potassium ions are located in between the Si_2O_7 groups for charge balance and exhibit K–O distances ranging from 2.743(2) to 3.021(2) Å. There are

Table 3
Selected bond lengths [Å] and angles for $K_3RESi_2O_7$ (*RE* = Gd, Tb, Dy, Ho, Er, Tm, Yb, Lu)

RE=	Gd	Tb	Dy	Ho	Er	Tm	Yb	Lu
RE(1)–O(1)	2.2788(13)	2.2626(13)	2.2525(14)	2.2420(14)	2.2324(15)	2.2228(14)	2.2116(18)	2.224(5)
RE(1)–K(1)	3.5731(3)	3.5572(4)	3.5509(4)	3.5428(5)	3.5361(4)	3.5303(4)	3.5239(6)	3.5372(11)
RE(2)–O(2)	2.3183(16)	2.3053(18)	2.2924(19)	2.283(2)	2.275(2)	2.2664(19)	2.261(3)	
RE(2)–K(1)	4.0108(6)	3.9927(6)	3.9835(7)	3.9708(9)	3.9635(7)	3.9564(7)	3.9446(9)	
RE(2)–K(3)	3.6074(6)	3.5964(7)	3.5893(7)	3.58015(15)	3.5746(6)	3.5716(7)	3.5600(7)	
Si(1)–O(1)	1.6154(13)	1.6125(14)	1.6119(15)	1.6089(19)	1.6114(16)	1.6129(14)	1.6123(19)	1.597(5)
Si(1)–O(2)	1.6231(17)	1.622(2)	1.625(2)	1.627(3)	1.626(2)	1.627(2)	1.626(3)	1.643(3)
Si(1)–O(3)	1.6605(11)	1.6613(12)	1.6611(13)	1.6596(17)	1.6618(15)	1.6633(14)	1.6618(19)	
Si(1)–K(1)	3.4273(4)	3.4108(5)	3.4052(5)	3.3979(7)	3.3909(6)	3.3842(5)	3.3465(12)	3.3430(7)
Si(1)–K(2)	3.6156(4)	3.5997(4)	3.5916(4)	3.5803(6)	3.5742(5)	3.5685(5)	3.5616(6)	3.6843(15)
Si(1)–O(3)–Si(1)	135.72(1)	135.31(18)	135.09(19)	135.1(2)	134.4(2)	134.29(19)	134.3(3)	180.0
O(1)–*RE*(1)–O(1)	87.83(7)	87.71(7)	87.70(8)	87.49(10)	87.65(8)	87.50(8)	87.36(10)	87.70(2)
O(1)–*RE*(1)–O(1)	88.81(5)	88.83(5)	88.93(5)	88.99(7)	88.91(6)	89.03(5)	89.14(7)	92.30(2)
O(1)–*RE*(1)–O(1)	94.77(7)	94.86(8)	94.67(8)	94.77(10)	94.77(8)	94.68980	94.59(11)	
O(1)–*RE*(1)–O(1)	175.03(6)	174.89(8)	175.02(8)	174.80(10)	174.91(9)	174.87(8)	174.84(11)	180.0(2)
O(2)–*RE*(2)–O(2)	80.409(8)	80.62(9)	80.42(10)	80.23(13)	80.22(11)	80.22(10)	80.23(13)	
O(2)–*RE*(2)–O(2)	82.82(6)	82.66(7)	82.81(7)	82.95(9)	82.96(8)	82.96(7)	82.95(10)	
O(2)–*RE*(2)–O(2)	135.10(3)	135.17(3)	135.11(3)	135.04(4)	135.03(4)	135.03(3)	135.04(5)	

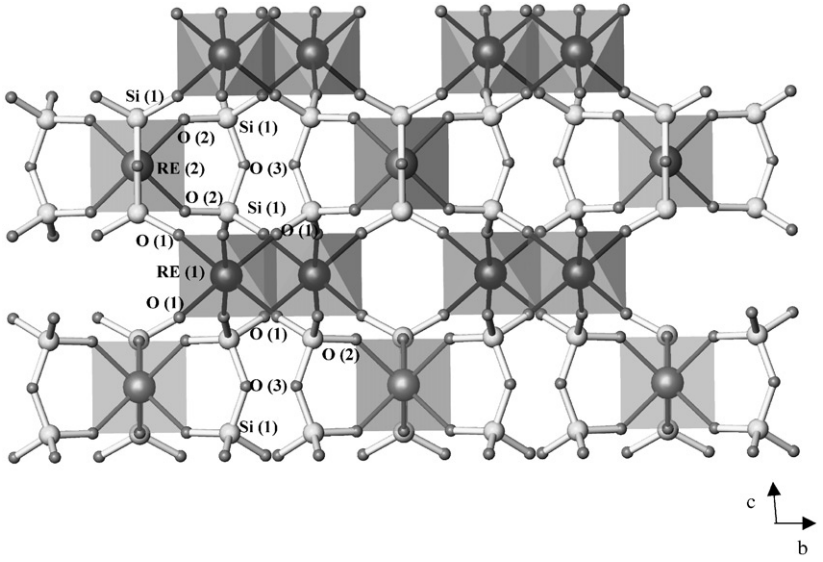

Fig. 2. Crystal structure of $K_3RESi_2O_7$ (*RE* = Gd, Tb, Dy, Ho, Er, Tm, Yb); the potassium ions are omitted for clarity.

three different potassium coordination environments in which the coordination number around the potassium varies from eight-coordinate for K(1), nine-coordinate for K(2), to six-coordinate for K(3).

The Si_2O_7 units are bent, Fig. 3a, with Si–O–Si angles ranging from 134.3(3) for Yb to 135.72(1) for Gd. The Si_2O_7 units connect to the rare earths, Fig. 4, such that the two "inner" O(2) oxygens are both connected to the same rare earth, supplying two out of six oxygens to its trigonal prismatic REO_6 coordination. The four "outer" O(1) oxygens are each connected to four different rare-earth cations, contributing one oxygen out of six to its octahedral REO_6 environment. Each Si_2O_7 unit is thus connected to five different rare-earth cations. This results in a structure consisting of layers containing all the trigonal prismatic rare earths that alternate with layers containing all the octahedrally coordinated rare earths Fig. 2.

The two coordination environments around the rare earths, octahedral and trigonal prismatic are shown in more detail in Figs. 5a and b, respectively. In Fig. 5a, it can be seen that the octahedral coordination sphere around the rare-earth cation is formed by oxygens originating on six different Si_2O_7 groups, while the trigonal prismatic coordination sphere, Fig. 5b, is formed from oxygens originating on only three different

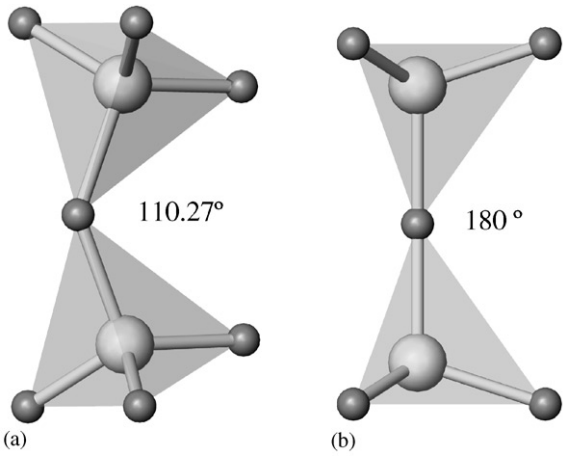

Fig. 3. Si_2O_7 units in: (a) $K_3RESi_2O_7$ (RE = Gd, Tb, Dy, Ho, Er, Tm, Yb) and (b) $K_3LuSi_2O_7$.

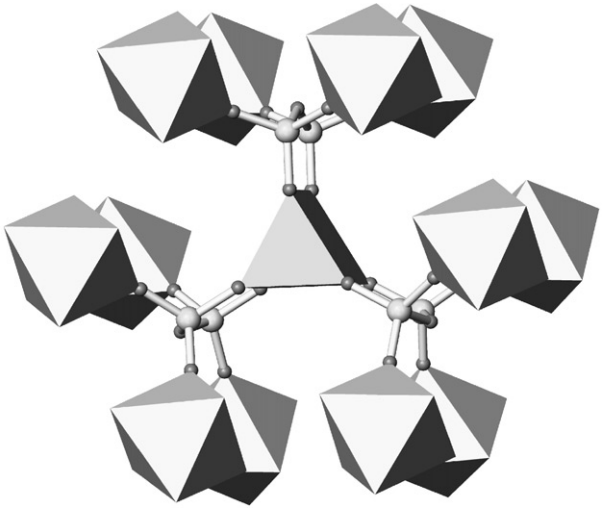

Fig. 4. Si_2O_7 connectivity in $K_3RESi_2O_7$ (RE = Gd, Tb, Dy, Ho, Er, Tm, Yb).

Si_2O_7 groups. While the octahedron is slightly distorted and has local D_{3d} symmetry, the trigonal prismatic environment has ideal D_{3h} symmetry. Both polyhedra are isolated in the structure and are connected via O–Si–O linkages to the other rare earths.

Only the structure of $K_3LuSi_2O_7$ differs from the one described above and crystallizes in a different space group, $P6_3/mmc$; it appears to have some similarity to that of $Ba_3NaSi_2O_7(OH)$ [23]. Unlike the previous structure, there is only one coordination environment for the rare earth in $K_3LuSi_2O_7$, octahedral. The a-lattice parameter is half that of the previous group, as a result of missing the trigonal prismatic site. The structure is still constructed from Si_2O_7 units that connect to the rare-earth cations, however, each Si_2O_7 unit is connected to six different rare-earth atoms. This is made possible by the fact that the Si_2O_7 unit has a Si–O–Si angle of 180° Fig. 3b. The structure, Fig. 6, consists of layers of isolated REO_6 octahedra that are connected via O–Si–O linkages. The potassium cations are located within the layers to provide charge balance. There are only two potassium positions, which are eight coordinate, rather than three potassium positions in the previous structure type. The K–O bond lengths are comparable and range from 2.8593(3) to 3.2976 Å.

It is interesting to note that the Si–O–Si angle does not change significantly for the different rare-earth cations, even though their size decreases steadily from Gd (0.94 Å) to Yb (0.87 Å). However, it appears that there is a critical rare-earth size, reached for lutetium, where a different structure type is favored. Based on simple-size arguments, we feel that the scandium (0.75 Å) and indium (0.80 Å) analogues should be isostructural with the lutetium (0.86 Å) structure, while the yttrium (0.90 Å) analogue should be isostructural with the first group.

We investigated the fluorescence properties of this series of rare earths. Hwang et al. [19] suggested that $K_3NdSi_2O_7$ might be a laser material due to the presence of neodymium in a distorted octahedral coordination environment. We tested all the crystals for fluorescence and found that $K_3TbSi_2O_7$ strongly fluoresces in the visible. Simply exposing the crystal to a hand-held UV source, the fluorescence could be easily seen with the naked eye. None of the other crystals showed fluorescence that could be detected visually and, consequently, only the fluorescence of $K_3TbSi_2O_7$ was further investigated. The fluorescence data are shown in Fig. 7 and four intense emissions can be observed at 485, 536, 583, and 617 nm. Based on previous investigations of the fluorescent properties of terbium [24,25], these transitions are most likely due to $^5D_4 -> {}^7F_6$, $^5D_4 -> {}^7F_5$, $^5D_4 -> {}^7F_4$, and $^5D_4 -> {}^7F_3$ transitions, respectively.

4. Conclusion

Single crystals of $K_3RESi_2O_7$ (RE = Gd, Tb, Dy, Ho, Er, Tm, Yb, Lu) were grown from a potassium fluoride flux and two similar, but different structure types were found. Silicates containing the larger rare earths, RE = Gd, Tb, Dy, Ho, Er, Tm, Yb crystallize in a structure that contains the rare-earth cation in both a slightly distorted octahedral and an ideal trigonal prismatic coordination environment, while in $K_3LuSi_2O_7$, containing the smallest of the rare earths, lutetium is found solely in an octahedral coordination environment. The optical properties of the silicates were investigated and $K_3TbSi_2O_7$ was found to strongly fluoresce in the visible.

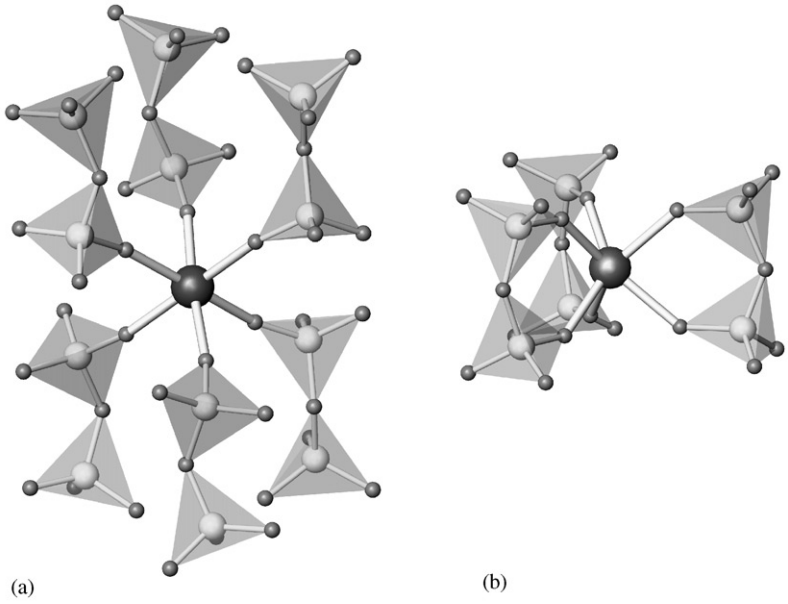

Fig. 5. Coordination environments of *RE* (Gd, Tb, Dy, Ho, Er, Tm, Yb): (a) elongated octahedron (D_{3d} symmetry) and (b) regular trigonal prism (D_{3h} symmetry).

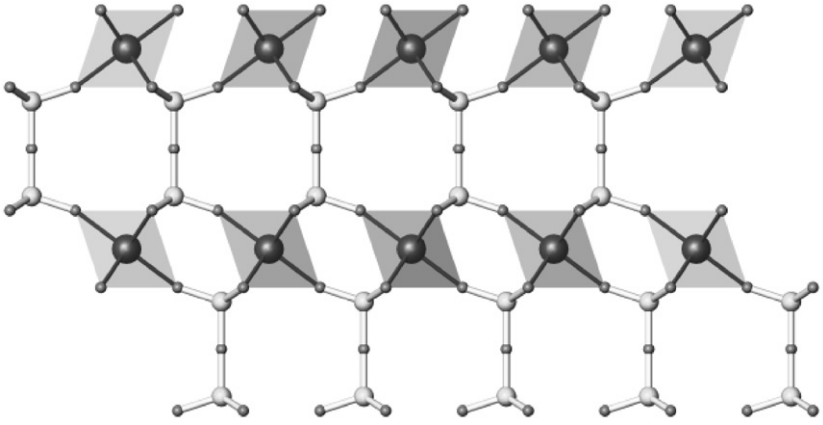

Fig. 6. Crystal structure of $K_3LuSi_2O_7$; the potassium ions are omitted for clarity.

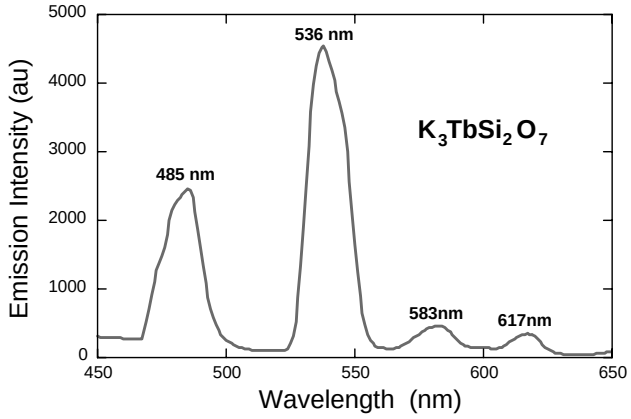

Fig. 7. Fluorescence spectrum of $K_3TbSi_2O_7$.

Acknowledgments

Funding for this research was provided by the National Science Foundation through Grant DMR: 0134156. Further details of the crystal structure investigations can be obtained from the Fachinformationszentrum Karlsruhe, 76344 Eggenstein-Leopoldshafen, Germany (fax (49) 7247-808-666; e-mail: crysdata@fiz.karlsruhe.ed) on quoting the depository numbers CSD-412521 (Gd); CSD-412522 (Tb); CSD-412523 (Dy); CSD-412524 (Ho); CSD-412525 (Er); CSD-412526 (Tm); CSD-412526 (Yb); CSD-412528 (Lu).

References

[1] N.A. Toropov, F. Galakhov, S.F. Konovalova, Izv. Akad. Nauk SSSR, Otd, Knim. Nauk 5 (1961) 739.
[2] A.I. Leonov, V.S. Rudenko, E.K. Keler, Izv. Akad. Nauk SSSR, Otd, Knim. Nauk 11 (1961) 1925.
[3] E.K. Keler, N.A. Godina, E.R. Savchenko, Izv. Akad. Nauk SSSR Otd, Knim. Nauk 10 (1961) 1735.
[4] N.A. Toropov, F. Galakhov, S.F. Konovalova, Izv. Akad. Nauk SSSR, Otd, Knim. Nauk 4 (1961) 539.
[5] N.A. Toropov, I.A. Bondar, A.N. Lazarevg, Yu.I. Smolin, Silicates of Rare-Earth Elements and Their Analogs, Nauka, Lenigrad. Otd., Lenigrad, USSR, 1971.
[6] J. Felsche, in: J.D. Dunitz (Ed.), Structure and Bonding, Vol. 13, Springer, Berlin, 1973, pp. 99–197.
[7] M.E. Fleet, X. Liu, J. Solid State Chem. 161 (2001) 166.
[8] A.V. Chicagov, B.N. Litvin, N.V. Belov, Kristallografiya 14 (1969) 119.
[9] B.A. Maksimov, B.N. Litvin, V.V. Ilyukhin, N. Belov, Kristallografiya 14 (1969) 498.
[10] M. Sebais, E.A. Pobedimskaya, O.V. Dimitrova, Kristallografiya 30 (1985) 802.
[11] R.A. Tamazyan, Y.A. Malinovskii, M.I. Sirota, V.I. Simonov, Kristallografiya 33 (1988) 1128.
[12] D.Y. Pushcharovskii, O.G. Karpov, E.A. Pobedimskaya, N.V. Belov, Dokl. Akad. Nauk SSSR 234 (1977) 1323.
[13] O.S. Filipenko, O.V. Dimitrova, L.O. Atovmyan, V.I. Ponomarev, Kristallografiya 33 (1988) 1122.
[14] O.S. Filipenko, G.V. Shilov, L.S. Leonova, N.S. Tkacheva, O.V. Dimitrova, V.I. Ponomarev, Russ. J. Coord. Chem. 25 (1999) 877.
[15] S.M. Haile, B.J. Wuensch, Acta Crystallogr. B 56 (2000) 773.
[16] S.M. Haile, B.J. Wuensch, T. Siegrist, R.A. Laudise, J. Crystal Growth 131 (1993) 352.
[17] V.I. Ponomarev, O.S. Filipenko, L.O. Atovmyan, Kristallografiya 33 (1988) 98.
[18] I.A. Bondar, T.F. Tenisheva, N.A. Toropov, Yu.F. Shepelev, Dokl. Akad. Nauk SSSR 160 (1965) 1069.
[19] M.S. Hwang, H.Y.P. Hong, M.C. Cheng, Y. Wang, Acta Crystallogr. C 43 (1987) 1241.
[20] S. Oishi, H. Minoru, Chem. Lett. (1991) 333–336.
[21] SMART Version 5.624, SAINT+ Version 6.02a and SADABS, Bruker Analytical X-ray Systems, Inc., Madison, Wisconsin, USA, 1998.
[22] G.M. Sheldrick, SHELXTL Version 5.1; Bruker Analytical X-ray Systems, Inc., Madison, Wisconsin, USA, 1997.
[23] O.S. Filipenko, E.A. Pobedimskaya, V.I. Ponomarev, N.V. Belov, Dokl. Akad. Nauk SSSR 200 (1971) 591.
[24] N.S. Hussain, Y.P. Reddy, S. Buddhudu, Mater. Lett. 48 (2001) 303.
[25] F.S. Kao, T.-M. Chen, J. Lumin. 96 (2002) 261.